Theoretical study of the ring opening of phosphirane and silirane: contrasting mechanisms of hydrogen migration †

Nguyen-Nguyen Pham-Tran,[a,b] Hue Minh Thi Nguyen,[a,c] Tamás Veszprémi[d] and Minh Tho Nguyen*[a]

[a] *Department of Chemistry, University of Leuven, Celestijnenlaan 200F, B-3001 Leuven, Belgium. E-mail: minh.nguyen@chem.kuleuven.ac.be*
[b] *Faculty of Chemistry, National University of HoChiMinh-City, Vietnam*
[c] *Faculty of Chemistry, University of Education, Hanoi, Vietnam*
[d] *Department of Inorganic Chemistry, University of Technology and Economics, Gellért tér 4, H-1521 Budapest, Hungary*

Received (in Cambridge, UK) 8th December 2000, Accepted 21st February 2001
First published as an Advance Article on the web 23rd March 2001

Ab initio quantum chemical calculations including HF, MP2, CCSD(T), CASSCF(12,12), CASPT2 and B3LYP methods with the basis sets ranging from 6-31G(d,p) to 6-311++G(3df,2p) were used to establish the contrasting mechanism of the ring–chain rearrangement of both three-membered phosphirane and silirane rings. It is confirmed that the phosphirane ring opening induced by C–P bond cleavage is accompanied by a hydrogen migration from C to P yielding vinylphosphine (H_2C=$CHPH_2$); both motions occur concertedly in a single step with an energy barrier of about 200 ± 15 kJ mol^{-1}. In contrast, the preferred ring opening of silirane by C–Si bond cleavage involves a downgrade hydrogen migration from Si to C giving rise to ethylsilylene (H_3C–CH_2–SiH) and is associated with a smaller energy barrier of 110 ± 15 kJ mol^{-1} (experimental: about 100 kJ mol^{-1} for substituted siliranes). There are no significant variations in transition structures geometries obtained either from single determinantal HF-based or multi-configurational CASSCF methods concerning the advance of H-transfer. The solvent effect is also probed using a polarizable continuum model (PCM). Full geometry optimizations within the continuum show that solvation enthalpies are rather small and do not modify the relative ordering of the energy barriers. The contrasting behaviour can be understood by the fact that ethylsilylene is a stable singlet isomer whereas singlet ethylphosphinidene ‡ has a high-energy content and does not exist as an equilibrium structure. Evolution of the Boys localized orbitals suggests that the H-atom migrates as a hydride from C to P and C to Si and as a proton from Si to C. Profiles of static polarizabilities and hardnesses along the IRC pathways are also constructed. In one case, the hardness profile does not follow the "principle of maximum hardness".

1. Introduction

Phosphiranes, phosphorus-containing analogues of cyclopropanes, are used as synthons for larger phosphorus heterocycles through a variety of ring expansions, and as complexing agents in coordination chemistry.[1] Tran-Huy, Mathey and co-workers[2–4] have shown experimentally that under thermal conditions,[2] or in the coordination sphere of transition metal complexes[3,4] such as $W(CO)_5$, a ring–chain inter-conversion is established between a phosphirane and a vinylphosphine. The rearrangement **1**→**2** formally involves an opening of the three-membered ring and a sigmatropic shift of a hydrogen or halogen atom (*cf.* eqn. (1), X = H, Cl and Br). In an earlier

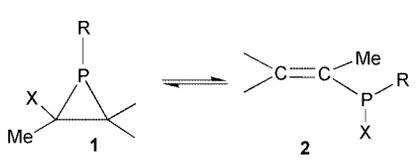

(1)

theoretical study,[5] we demonstrated that the process **1**→**2** is an energetically concerted process in which the C–P bond breaking in **1** and the H-shift from C to P occur in a single transition structure. The conversion of **1** to **2** was also found to be the most favoured process among many possible transformations of phosphirane[5] even though it is associated with a high energy barrier (235 kJ mol^{-1} computed at the QCISD(T)/6-311G(d,p)+ZPE level of MO theory). An interesting feature here is that the hydrogen atom migrates from a more electronegative C center to a less electronegative P.

With regards to the silicon analogue (silacyclopropane or silirane), earlier mass spectrometric studies[6] indicated that ring opening of silirane might not follow a similar pattern. In fact, earlier *ab initio* calculations[7] on the [C_2SiH_6] potential energy surface showed that although the parent silirane **SiR** also undergoes a concerted ring–chain rearrangement with C–Si bond cleavage, it prefers a downgrade hydrogen migration from Si to C yielding ethylsilylene **SiP2** as the primary product rather than forming either vinylsilane **SiP1** [the Si-counterpart of **2**, eqn. (2)] or other isomers such as CH_3–Si–CH_3, H_2Si=$CHCH_3$ and CH_2=$SiHCH_3$, even though the latter are thermodynamically more stable than ethylsilylene.[7] A subsequent theoretical

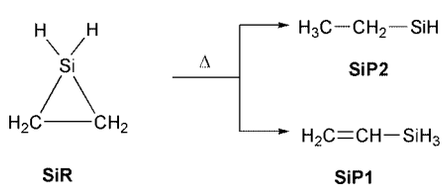

(2)

† Optimised geometries for the compounds studied are available as supplementary data. For direct electronic access see http://www.rsc.org/suppdata/p2/b0/b009918j/

‡ The IUPAC name for ethylphosphinidene is ethylphosphanediyl.

 DOI: 10.1039/b009918j

study[8] appeared to confirm these results suggesting the formation of **SiP2**. Accordingly, the energy barrier associated with the **SiR→SiP2** conversion was computed to be 109 kJ mol^{-1} using QCISD(T)/6-311G(d,p)+ZPE energies[7] or 103 kJ mol^{-1} using CASSCF(12,12)/CASPT2/6-31G(d,p) wavefunctions.[8] In addition, these computed barriers compared well with that obtained by kinetic measurements.[6] Although the hydrogen transfer from an electropositive Si center to a more electronegative C could usually be expected, the observed downgrade hydrogen migration creating a divalent silicon center constitutes a peculiar feature. The ring-opening that breaks the C–C bond giving methylsilene (CH_3–SiH=CH_2) was not observed.

Taken together, the results summarized above clearly point out the contrasting behaviour of both P and Si three-membered rings in their unimolecular reactivities. Nevertheless, the fact that the theoretical results reported earlier[5,7,8] for both systems were done at different levels of theory, does not allow a consistent comparison of the above mentioned barriers to be made. On the other hand, the rearrangement **SiR→SiP1** was considered in ref. 7 but not in ref. 8; therefore a confident differentiation between the two pathways could not be made.

In view of the interesting variance of behaviour and properties of analogous three-membered cycles,[5,7–12] we set out to address the problem again by performing a series of uniform and reliable calculations on the pathways given in both eqns. (1) and (2), to obtain comparable geometrical and energetic parameters. In addition, an attempt to emphasise the mechanistic difference has been made in analysing various electronic properties of the supersystems along the intrinsic reaction pathways.

2. Methods of calculation

Quantum chemical calculations were carried out using the Gaussian 98[13] and Molcas-4[14] program packages. The geometries of the studied structures were fully optimized at different levels of molecular orbital theory including the Hartree–Fock (HF), second order perturbation theory (MP2), and the complete active space self-consistent-field with active spaces of 8-electrons-in-8-orbitals (referred to hereafter as CAS(8,8)), as well as using the hybrid functional B3LYP method of density functional theory.[15] Second derivatives of energies and harmonic frequencies were calculated for all considered structures to establish whether they are either real minima or transition structures on the potential energy super-surface at both MP2 and B3LYP levels. The identity of each transition structure was confirmed by intrinsic reaction coordinate (IRC) computations. To estimate further the influence of higher excitations and/or multi-reference character of the corresponding wavefunctions on the activation parameters, single point electronic energy computations using the coupled-cluster theory including all single and double and perturbative correction for triple excitations (CCSD(T)), as well as second order perturbation theory based on complete active space wavefunctions (CASSCF(12,12)/CASPT2), were also carried out using different optimized geometries. Different atomic basis functions including the 6-31G(d,p), 6-311++G(d,p) and 6-311++G(3df,2p) sets have been employed. The variations of some electronic properties of the supersystems such as the Boys-localized orbitals, hardnesses and static polarizabilities along the IRC pathways were also evaluated. To probe the effect of the bulk solvent on the relative energies, a polarizable continuum model (PCM)[16,17] approach has also been applied at the HF and B3LYP/6-31G(d,p) level of theory. The geometries were also re-optimised with the presence of a solvent continuum. Throughout this paper, bond lengths are given in ångströms, bond angles in degrees, total energies in hartrees, zero-point vibrational and relative energies in kJ mol^{-1}.

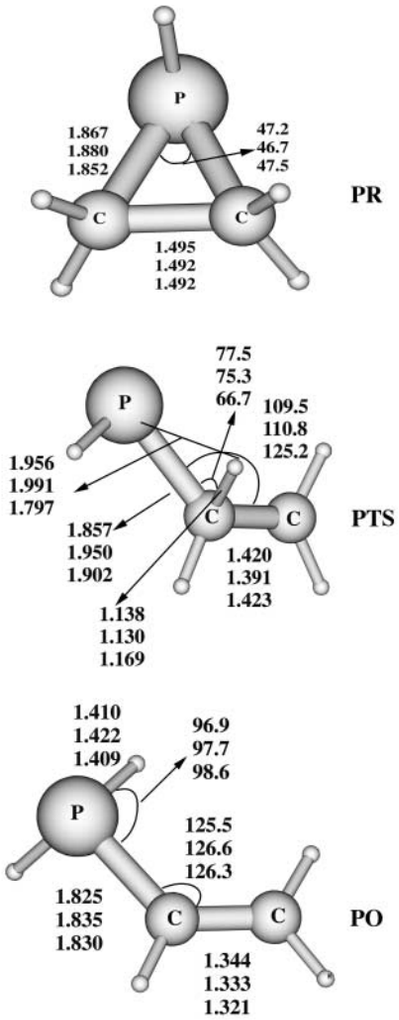

Fig. 1 Selected geometrical parameters of phosphirane **PR**, the transition structure **PTS** for ring–chain rearrangement and vinylphosphine **PO**. The values are: upper: MP2, middle: B3LYP and lower: CASSCF(8,8) using the 6-311++G(d,p) basis set.

3. Results and discussion

For each of the transition structures considered we have constructed the intrinsic reaction coordinate (IRC) pathway in order to verify its identity, to make sure that there is no other intermediate on the path, and perhaps more interestingly to determine the geometries of the points on which variations of electronic properties of the supersystem could be monitored. The IRC paths obtained using either HF and MP2 levels with the 6-31G(d,p) basis set confirm in fact that the conversion of a three-membered ring to its open-chain isomer is a single step. We will first present the results concerning the rearrangements of phosphirane and silirane and followed by an analysis of some electronic properties along the IRC paths.

Rearrangement of phosphirane

Fig. 1 displays the selected geometrical parameters of the parent phosphirane ring **PR**, its open isomer vinylphosphine **PO** and the transition structure for rearrangement **PTS**, optimised using three different quantum chemical methods namely the MP2, B3LYP and CAS(8,8) in conjunction with the 6-311++G(d,p) basis set. The full sets of MP2-geometries are given in the Supplementary Information. Calculated energies using various levels of theory are summarised in Table 1. The ring opening of the unsubstituted phosphirane was investigated in detail in an earlier theoretical study[5] in which the geometries were optimised at the MP2/6-31G(d,p) level, and the relative energies estimated from single-point electronic energy com-

Table 1 Calculated energies of the phosphirane system using different levels of theory

Level	Geometry	Total energy (**PR**)/hartree	ΔE (**PO**)[a]/ kJ mol^{-1}	ΔE (**PTS**)[a]/ kJ mol^{-1}
MP2/6-31G(d,p)	MP2/6-31G(d,p)	−419.73680	28	272
B3LYP/6-31G(d,p)	B3LYP/6-31G(d,p)	−420.54800	11	232
QCISD(T)/6-311G(d,p)[b]	MP2/6-31G(d,p)	−419.84934	10	235
MP2/6-311++G(d,p)	MP2/6-11++G(d,p)	−419.79700	23	265
MP2/6-311++G(3df,2p)	MP2/6-11++G(d,p)	−419.87750	25	254
B3LYP/6-311++G(d,p)	B3LYP/6-311++G(d,p)	−420.59229	3	226
CAS(8,8)/6-311++G(d,p)	CAS(8,8)/6-311++G(d,p)	−419.44041	5	220
CCSD(T)/6-311++G(d,p)	CAS(8,8)/6-311++G(d,p)	−419.85195	14	228
CCSD(T)/6-311++G(d,p)	MP2/6-311++G(d,p)	−419.85255	11	230
CCSD(T)/6-311++G(d,p)	B3LYP/6-311++G(d,p)	−419.85250	11	232
CASPT2/6-311++G(d,p)[c]	CAS(8,8)/6-311++G(d,p)	−419.96401	1	210

[a] Including zero-point corrections. the ZPE's obtained from B3LYP/6-31G(d,p) computations are: **PR**: 166, **PO**: 157 and **PTS**: 154 kJ mol^{-1}. [b] Taken from ref. 5. [c] Based on the CASSCF(12,12) references.

Table 2 Rotational constants (MHz) of the phosphirane

Method	*A*	*B*	*C*
MP2/6-31G(d,p)	20392	9732	7626
B3LYP/6-31G(d,p)	20208	9549	7503
MP2/6-311++G(d,p)	20217	9759	7631
B3LYP/6-311++G(d,p)	20226	9607	7538
CASSCF/6-311++G(d,p)	19886	9809	7597
Experimental[a]	20094	9801	7634

[a] Microwave data taken from ref. 18.

putations at the quadratic configuration interaction (QCI) QCISD(T)/6-311G(d,p) level. For the purpose of comparison, the QCI values are also listed in Table 1. According to earlier results,[5] the phosphirane–vinylphosphine interconversion is by far the most favoured process among numerous possible transformations of phosphirane.

As expected, there are some significant variations on the geometrical parameters of the structures considered in going from one level to another. For phosphirane **PR**, the B3LYP method provides larger C–P distances relative to the MP2 whereas the CAS(8,8) gives much shorter length (up to 0.15 Å in either direction). These bring about however rather small fluctuations in the rotational constants (Table 2). Both MP2 and B3LYP levels reasonably reproduce these molecular parameters as compared with the values derived from microwave spectroscopy.[18] For vinylphosphine **PO**, the variations on both C=C and C–P distances are much smaller amounting up to only 0.02 Å. We refer the reader to refs. 5, 19 and 20 for detailed theoretical analyses of both isomers.

Of particular interest is the transition structure **PTS**. Because it does not have any symmetry, selection of the orbitals to be included in the active space is not unequivocal. However, the selected CAS(8,8) space seems to be large enough to include the main orbitals involved in the reorganisation process. All three methods employed confirm the concerted character of the rearrangement in which the ring opening is accompanied by a hydrogen migration from the central C atom to the P. Compared with both MP2 and B3LYP methods, the CAS(8,8) method tends to suggest a more compact framework for the H-migration with a slightly longer C···H distance and a much shorter P···H distance (up to 0.2 Å) while being associated with a wider CCP angle. Nevertheless, the results are internally consistent suggesting that while the C–H bond is marginally stretched, the new P–H bond is also marginally formed at the TS.

Results listed in Table 1 indicate the following points: (i) extension of the basis functions or incorporation of larger amounts of electron correlation in wavefunctions tends to reduce the energy barrier, namely by 18 kJ mol^{-1} in going from MP2/6-31G(d,p) to MP2/6-311++G(3df,2p) and by 35 kJ mol^{-1} from MP2 to CCSD(T) with the 6-311++G(d,p) basis; (ii) change in the geometries does not make any significant change in the barrier. Use of three distinct sets of optimised geometries, namely MP2, B3LYP and CAS(8,8), induces a fluctuation of at most 4 kJ mol^{-1} at the single point CCSD(T) level; (iii) the B3LYP level provides us with results quite close to the CCSD(T) counterpart, and (iv) the CASPT2 level delivers the largest reduction of the energy barrier, up to 20 kJ mol^{-1}. Nevertheless, analysis of the CASSCF wavefunctions of **PTS** indicates that the Hartree–Fock reference and the doubly excited configuration from HOMO to LUMO have weights of 0.85 and 0.10, respectively. This strongly suggests the non-biradical character of the ring-opening motion. Taking both effects of basis set completeness and electron correlation into account, the lower limit of the energy barrier for rearrangement of phosphirane **PR** could be estimated at about 200 ± 15 kJ mol^{-1}. This is in line with the fact that the phosphirane–vinylphosphine interconversion is a thermally demanding process.[2]

Extensive calculations on the ethylphosphinidene isomer (CH_3CH_2P) formally resulting from a ring-opening of phosphirane with a H-migration from P to C, confirm that: (i) at the lower levels of theory (HF and MP2 using 6-31G(d,p)), a C_s-symmetry structure exists as a shallow local minimum. Single point electronic energies at the higher CCSD(T) level indicate that the C_s-C_2H_5P structure is a high energy species lying about 190 kJ mol^{-1} above phosphirane, and (ii) when geometry optimisations were carried out at the CCSD(T) level, ethylphosphinidene however no longer exists as a discrete stationary point on the closed-shell singlet energy surface but actually collapses into *C*-methylphosphaethene (H_3C–CH=PH). Nevertheless, we were not able to establish any formal connection between **PR** and H_3C–CH=PH through a single transition structure. Therefore it appears reasonable to admit that vinylphosphine is the sole product of a single step ring-opening of phosphirane. We refer the reader again to ref. 5 for the various pathways in other parts of the potential energy surface.

In an attempt to evaluate the effect of solvent on the energy data, calculations using the continuum model have also been carried out. First we have considered the simple self-consistent reaction field model (SCRF)[13] using single point B3LYP/6-31G(d,p) with gas phase geometries. It turns out that the free energies of solvation of all three structures **PR**, **PO** and **PTS** are similar but positive (ΔG_{sol} being around +18–20 kJ mol^{-1}), implying that they are destabilized upon electrostatic interaction with the solvent. Subsequent computations using the better polarizable continuum model[16–17] in conjunction with the HF/6-31G(d,p) level) indicate that either in aqueous or DMSO solution, while both equilibrium structure **PR** and transition structure **PTS** have small but negative free energies of solvation (ΔG_{sol} being −7 kJ mol^{-1}), the corresponding value for **PO** is

small but positive (ΔG_{sol} being +2 kJ mol^{-1}). The consequence is that there is virtually no change in the energy barrier following a non-specific solvation of the supersystem by a solvent continuum.

To gain additional information as to whether the changes in the nuclear configurations of the stationary points in solvent could make some more significant changes in the barrier, we have also re-optimized their geometries with the presence of a continuum (water and DMSO). Fig. 2 displays the main parameters of the **PTS** making use of the HF/6-31G(d,p) method without (gas phase) and with a solvent continuum (water) in the framework of the PCM method.[16,17] It is apparent that the structural modifications upon solvation in the aqueous continuum are rather small, and more importantly, the shape of the TS remains unchanged. Overall these changes induce somewhat larger solvation free energies for both **PR** and **PTS**, namely −14 and −11 kJ mol^{-1}, respectively. For its part the continuum effect on vinylphosphine **PO** is tiny, being less than +1 kJ mol^{-1}. This means that the energy barrier is expected to be increased by merely 3 kJ mol^{-1} upon solvation either in aqueous or DMSO media. Thus, there is no significant solvent effect on phosphirane rearrangement when a less polar solvent than DMSO should be used. It should however be stressed that in the PCM treatment, the Coulomb electrostatic interactions constitute the dominant contributions into the solvation energies. We could not rule out an involvement of other terms such as specific interactions through hydrogen bonds between substrates and solvent molecules.[21]

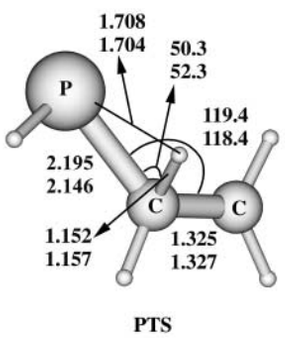

Fig. 2 Selected geometrical parameters of the transition structure **PTS** without and with the presence of a solvent continuum. The entries are: upper: gas phase HF/6-31G(d,p), and lower: aqueous solution HF-PCM/6-31G(d,p).

Rearrangement of silirane

For the sake of completeness, let us first look again at the various transformations on the [C_2SiH_6] potential energy surface. Fig. 3 shows the schematic potential energy curves linking different isomers obtained from QCISD(T)/6-311G(d,p)+ZPE based on MP2/6-31G(d,p) optimized geometries.[7] It appears that while the **SiR**–**SiTS1**–**SiP1** path contains an energy-demanding step, the **SiR**–**SiTS2**–**SiP2** one effectively corresponds to the lowest energy pathway even though the silylene intermediate **SiP2** is the thermodynamically least stable of the isomers considered. Here we consider further these two ring-opening reaction paths of silirane. Fig. 4 displays the selected geometrical parameters of the unsubstituted silirane **SiR**, both open isomers **SiP1** and **SiP2**, as well as the corresponding transition structures for ring opening **SiTS1** and **SiTS2**, respectively [*cf*. eqn. (2)]. While both MP2 and B3LYP geometries were obtained with the 6-311++G(d,p) basis sets, the CAS(8,8) values were determined using the 6-31G(d,p) set. Due to some difficulties encountered during the optimization processes, the CAS(8,8) values with the larger basis could not be completely derived. The full set of MP2-geometries are again given in the Supplementary Information. Table 3 lists the calculated total and relative energies of the five [C_2SiH_6] stationary points considered at different levels of theory. For the following discussion, unless otherwise noted, we refer to the values obtained from CCSD(T)/6-311++G(3df,2p)+ZPE computations.

For the three equilibrium structures, the variations with respect to the methods are the largest for the C–Si bond distances, amounting up to 0.05 Å in ethylsilylene **SiP2**. The Si–H bonds also experience large fluctuations on their calculated distances (up to 0.03 Å). Regarding their relative stabilities, it is

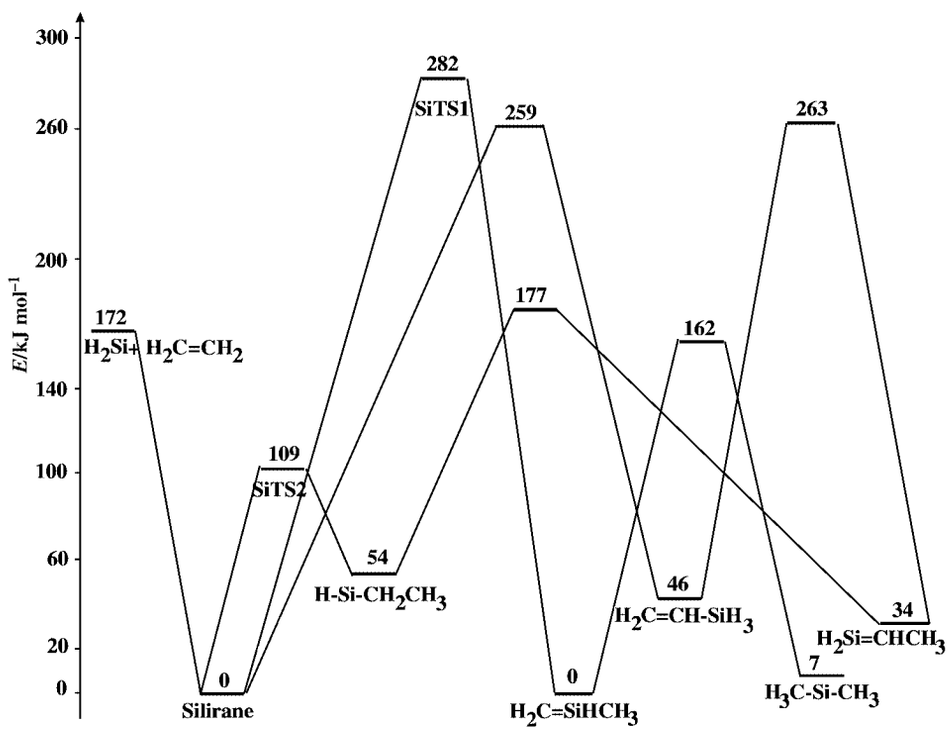

Fig. 3 Schematic potential energy diagram illustrating various reactions of the C_2SiH_6 isomers. Relative energies obtained from QCISD(T)/6-311G(d,p)//MP2/6-31G(d,p)+ZPE level of theory.[7]

Table 3 Calculated energies of the silirane system using different levels of theory

Level[a]	Total energy **SiR**[b]	Relative energies[c]			
		SiTS1	**SiP1**	**SiTS2**	**SiP2**
MP2/6-31G(d,p)	−368.48086	225	−35	115	61
B3LYP/6-31G(d,p)	−369.27805	249	−45	95	48
CASSCF(8,8)/6-31G(d,p)	−369.13610	251	−139	50	21
MP2/6-311++G(d,p)	−368.54060	251	−36	114	70
B3LYP/6-311++G(d,p)	−369.32147	218	−48	98	51
CASPT2(12,12)/6-311++G(d,p)[d]	−368.71094	256	−43	113	75
CCSD(T)/6-31G(d,p)[e]	−368.53451	240	−45	108	45
CCSD(T)/6-311++G(d,p)[e]	−368.59773	236	−46	107	54
CCSD(T)/6-311++G(3df,2p)[e]	−368.67067	241	−42	110	58

[a] Based on optimised geometries at the level indicated, unless otherwise noted. [b] Total energies of silirane **SiR** given in hartree. [c] Relative energies with respect to silirane **SiR** given in kJ mol^{-1} including the zero-point corrections. The ZPE's in kJ mol^{-1} obtained from B3LYP/6-31G(d,p) are: **SiR**: 183, **SiTS1**: 168, **SiP1**: 176, **SiTS2**: 180 and **SiP2**: 186. [d] Based on CAS(8,8)/6-31G(d,p) geometries. [e] Based on MP2/6-311++G(d,p) geometries.

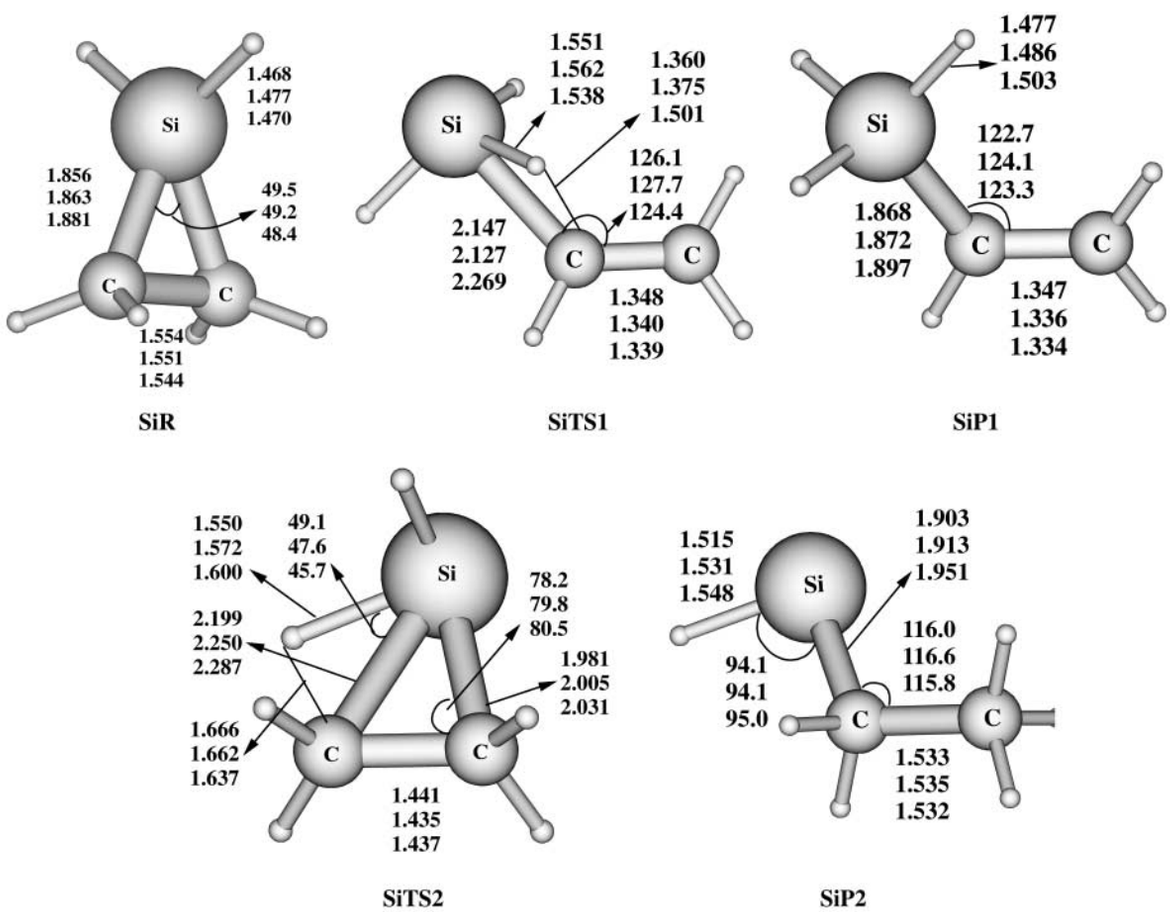

Fig. 4 Selected geometrical parameters of stationary points related to the ring-chain rearrangement of silirane **SiR**. The entries are: upper: MP2/6-311++G(d,p), middle: B3LYP/6-311++G(d,p) and lower: CASSCF(8,8)/6-31G(d,p).

confirmed that vinylsilane **SiP1** is the most stable isomer, lying 42 and 100 kJ mol^{-1} below **SiR** and **SiP2**, respectively; these values are quite close to the QCISD(T) counterparts given in Fig. 3. The relationship between **SiR** and **SiP1** is thus at variance with that discussed in the preceding section for the phosphorus analogues **PR**–**PO**. Silyl is apparently a better group than phosphino at stabilizing the alkene moiety. In this respect, singlet silylene **SiP2** is also a low-lying isomer being only 60 kJ mol^{-1} above the ring, bearing in mind that the species containing a divalent silicon atom are particularly stable.[22] As mentioned above, the P-counterpart of **SiP2**, namely singlet ethylphosphinidene, does not exist as an equilibrium structure. The phosphinidene functional group (R–P) is known to exhibit a triplet ground state unless the substituent R is a strong π-donor group.[23,24]

The transition structure **SiTS1** linking the three-membered ring **SiR** with vinylsilane **SiP1**, is the silicon counterpart of **PTS** described above. **SiTS1** was not considered in ref. 8. Comparison of the geometries of both **PTS** and **SiTS1** reveals a few remarkable differences, namely: (i) the ring is more widely opened in **SiTS1** and (ii) starting from the ring, the hydrogen migration is markedly more advanced in **SiTS1**, in the sense that the C–H bond is practically broken (1.5 compared to 1.08 Å) and the Si–H bond is virtually formed (1.55 compared to 1.50 Å in the product), in clear contrast with the situation in **PTS**. Thus **PTS** can be regarded as closer to the ring **PR** and **SiTS1** closer to the open isomer **SiP2**. In view of the relative energies stated above, apparently neither system obeys the Hammond postulate. The energy barrier for the transformation **SiR**–**SiP1** through **SiTS1** remains high, amounting to about

240 kJ mol^{-1} (Table 3; see also Fig. 3), which is slightly higher than the value for the **PR**–**PTS**–**PO** process (Table 1).

The transition structure-**SiTS2** connecting silirane-**SiR** to silylene-**SiP2**, was considered in both refs. 7 and 8 in which its MP2/6-31G(d,p) and CAS(4,4)/6-31G(d,p) geometries were reported, respectively. By and large, the latter is comparable to those obtained from B3LYP and CAS(8,8) levels shown in Fig. 3. The features of this TS were abundantly described in earlier studies[7,8] and thus warrant no additional comments. We only note that it is geometrically closer to silirane with a rather small opening of the three-membered ring; the CCSi bond angle moves from 65 to 80 degrees inducing a small stretching of 0.2 Å of the broken C–Si bond. The migration of the hydrogen from Si to C atom also implies a strong bending of the HSiC angle, putting it toward the middle region of the broken C–Si bond. Nevertheless, the migrating hydrogen remains more attached to silicon than to carbon even though the C–H binding energy is larger than that of Si–H.[25] This is in line with the character of **SiTS2** being closer to silirane than to its rearranged isomer. The energy barrier associated with **SiTS2** with respect to silirane **SiR** is computed to lie within a small range of values, from 100 to 110 kJ mol^{-1} using different methods. In fact the best estimate here (*cf*. Table 3) amounts to 110 kJ mol^{-1} from CCSD(T)/6-311++G(3df,2p)+ZPE and 113 kJ mol^{-1} from CASPT2(12,12)/6-311++G(d,p). A barrier of 109 and 103 kJ mol^{-1} was previously derived from QCISD(T)/6-311G(d,p)+ZPE[7] and CASPT2-(12,12)/6-31G(d,p)+ZPE[8] treatments, respectively, and they concur with the present results using larger atomic functions. The fact that within a certain basis set, the CASPT2 results are quite close to the MP2 counterparts, clearly indicates that the CAS wavefunctions are dominated by the HF references.

On the one hand, such a barrier turns out to be far smaller than that of 240 kJ mol^{-1} stated above for the alternative ring opening **SiR**–**SiTS1**–**SiP1**. On the other hand, it is consistent with the experimental estimates of 100–120 kJ mol^{-1} evaluated from kinetic measurements for the ring opening processes of substituted siliranes.[6] Overall, the present results confirm the preference of silirane undergoing a ring opening at a C–Si bond accompanied by a downgrade hydrogen migration from Si to C of the same bond forming a divalent silicon species. Thus, the ring opening of silirane-**SiR** accompanied by a hydrogen migration from Si to C is intrinsically favoured over that from C to Si. The shift from Si to C follows the normal direction of hydrogen migration and is in line with the relative electronegativities of both atoms.

Variations of electronic properties along intrinsic reaction coordinate pathways

As mentioned above, the IRC pathways starting from **PTS**, **SiTS1** and **SiTS2** were constructed making use of HF and MP2 wavefunctions and the 6-31G(d,p) basis set. Using the geometries of the points located on these pathways, the localized molecular orbitals (LMO) according to the Boys procedure,[26] total hardness (χ)[27] and static polarizability (α) were calculated. For the sake of clarity, Fig. 5 displays only the LMO centroids of charge corresponding to two electron pairs involved in the rearrangement. The LMOs of **PTS** have been analysed in a previous study[7] but are also given in Fig. 5 for the purpose of comparison. The profiles of energy, hardness and static polarizability are illustrated in Fig. 6.

Although the evolution of LMO centroids of charge is not clear-cut and unequivocal, it suggests the following reorganization of electron pairs.

PTS: (i) σ(C–H) **PR**→σ(P–H) **PO**
(ii) σ(C–P) **PR**→π(C–C) **PO**
SiTS1: (i) σ(C–H) **SiR**→σ(Si–H) **SiP1**
(ii) σ(C–Si) **SiR**→π(C–C) **SiP1**
SiTS2: (i) σ(Si–H) **SiR**→n(Si) **SiP2**
(ii) σ(C–Si) **SiR**→σ(C–H) **SiP2**

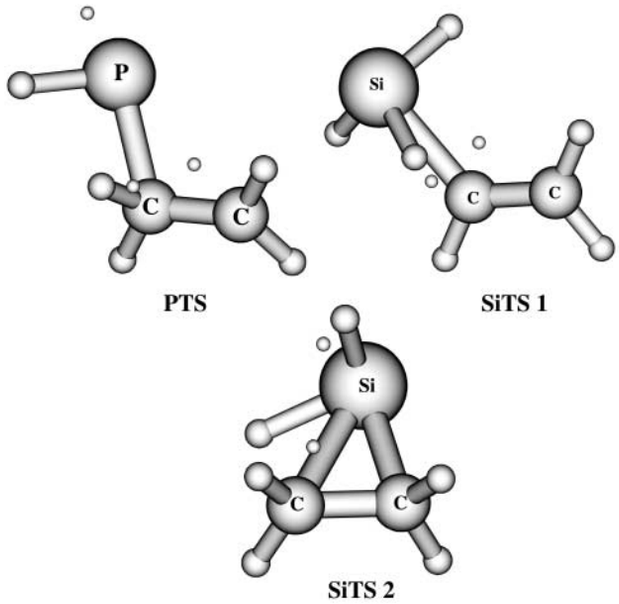

Fig. 5 Charge centroids of Boys localized orbitals in **PTS**, **SiTS1** and **SiTS2**. HF/6-31G(d,p) wavefunctions were used along the IRC paths.

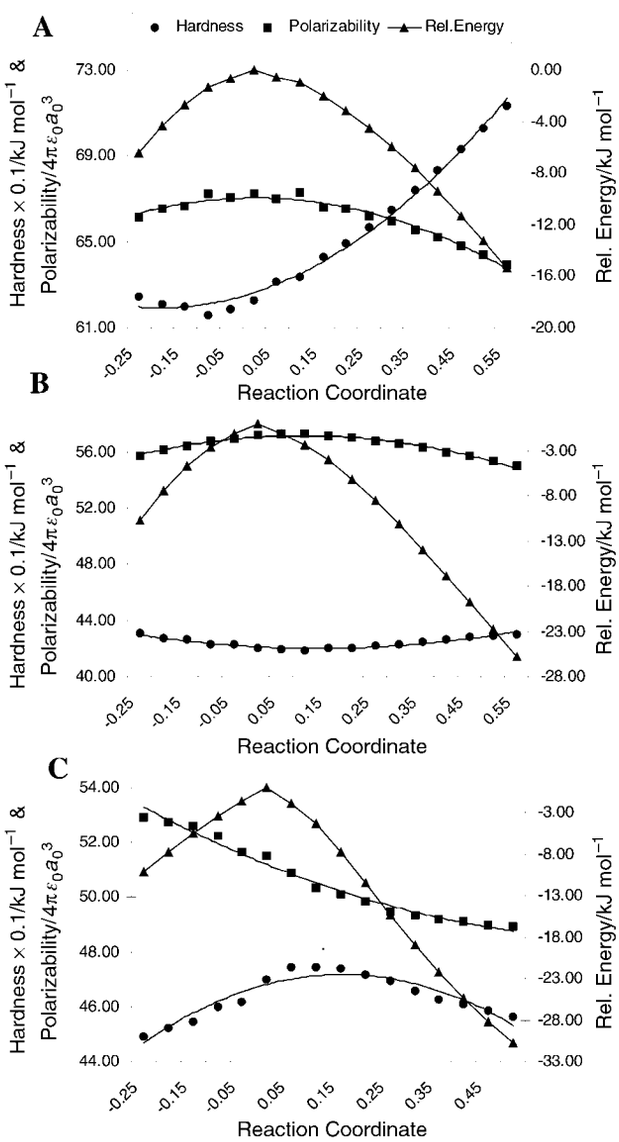

Fig. 6 Profiles of relative energy (E/kJ mol^{-1}), hardness (χ/kJ mol^{-1}) and static polarizability (α, $4\pi\varepsilon_0 a_0^3$) along three IRC ring-opening pathways using B3LYP/6-31G(d,p). **A**: phosphirane *via* **PTS**, **B**: silirane *via* **SiTS1**, and **C**: silirane *via* **SiTS2**.

In both **PTS** and **SiTS1**, the H-atom seemingly migrates as a hydride with the electron pair of the C–H bond, at least in the first **PR**–**PTS** part of the reaction path. In contrast, **SiTS2** apparently involves the migration of a proton which scrambles between two electron pairs. Perhaps such behaviour variation in part causes a difference in the corresponding activation energies.

In recent years, the reactivity descriptors based on density functional theory (DFT) have been found to be very useful for rationalizing reaction mechanisms.[27,28] In particular, the possibility of defining a profile of global hardness (χ) along a IRC path has been demonstrated.[29–32] The interest of such profiles is that they form a direct way of testing the "principle of maximum hardness" (PMH).[27,33] Because there is an inverse relationship between hardness and static polarizability,[34] a "principle of minimum polarizability" (PMP) has also been put forward.[35] Accordingly, the larger the hardness, the smaller the polarizability and the more stable the molecular system. In other words, a transition structure corresponds to a point having a maximum energy, a minimum hardness and a maximum polarizability.

The global hardness is defined as: $\chi = (IE - EA)/2$, where IE and EA are the first vertical ionization energy and electron affinity of the molecule, respectively.

The static polarizability is calculated as the arithmetic average of the three diagonal elements of the polarizability tensor: $\alpha = (\alpha_{xx} + \alpha_{yy} + \alpha_{zz})/3$ in which the α_{ii} ($i = x, y, z$) values are obtained using the finite field method.

The profiles shown in Fig. 6 point out some interesting results: (i) as expected, the hardness of **SiTS2** (0.47×10^{-1} kJ mol^{-1}) is larger than that of **SiTS1** (0.4347×10^{-1} kJ mol^{-1}) in line with the postulate mentioned above that the larger the hardness, the more stable the molecular system[27,34] (Fig. 6B and 6C); (ii) in the phosphirane ring opening *via* **PTS** (Fig. 6A), the calculated profiles indicate a shallow polarizability maximum and hardness maximum in the near saddle region, but the extreme positions do not coincide with that of the energy; (iii) in the silirane case with **SiTS1** (Fig. 6B), a shallow polarizability maximum in the saddle region could be found but no clear-cut minimum hardness could be located; (iii) in the second silirane reaction with **SiTS2** (Fig. 6C), while no polarizability maximum could be identified in the saddle region, the hardness profile is rather perplexing! As a matter of fact, it shows a hardness maximum in the saddle region rather than a minimum, in disagreement with the PMH mentioned above. For the time being, we only wish to report this intriguing finding with the hope of stimulating further detailed studies to figure out the reason for such a discrepancy.

Concluding remarks

In the present theoretical paper, we have pointed out the remarkably contrasting behaviour of phosphirane and silirane in their ring–chain rearrangements. While the ring opening of phosphirane yielding vinylphosphine is mainly associated with a hydrogen migration from C to P and a large barrier height of about 200 kJ mol^{-1}, the preferred ring opening of silirane involves a downgrade hydrogen migration from Si to C giving rise to ethylsilylene. The difference can be found in the inherent properties of both phosphorus and silicon atoms. Bearing in mind that both P and Si atoms are much less electronegative than C, the downgrade silirane rearrangement follows thus a more normal trend of hydrogen migration (from a less to a more electronegative center) and is therefore energetically less demanding; the energy barrier being about 110 kJ mol^{-1}. In this case, Boys localized orbitals suggest a proton migration whereas a hydride migration is likely to be involved in higher energy ring openings. These results are also consistent with earlier experimental and theoretical findings. In addition, the difference in the ring opening mechanism between both cyclic analogues can also be understood by the intrinsic difference between P and Si compounds. While the dicoordinated silicon isomer (alkylsilylene) is quite stabilized, the monocoordinated phosphorus counterpart (singlet alkylphosphinidene) has high energy content and simply does not exist as a discrete species. The obtained results highlight again the fact that strained cyclic compounds are perfectly able to undergo ring–chain rearrangements under mild conditions without needing to pass through biradical intermediates.[36,37]

Acknowledgements

This study was realized within the framework of a Bilateral Cooperation Agreement between the Governments of the Flemish Community of Belgium and Hungary (project BIL03/98). The Leuven group is also indebted to the FWO-Vlaanderen and the KULeuven concerted research action program (GOA). The Budapest group thanks the OTKA for financial support (project T034768).

References

1 F. Mathey, *Chem. Rev.*, 1990, **90**, 997.
2 S. Haber, P. Le Floch and F. Mathey, *J. Chem. Soc., Chem. Commun.*, 1992, 1799.
3 N. H. Tran Huy and F. Mathey, *Synlett*, 1995, 353.
4 N. H. Tran Huy and F. Mathey, *J. Org. Chem.*, 2000, **65**, 652.
5 M. T. Nguyen, L. Landuyt and L. G. Vanquickenborne, *J. Chem. Soc., Faraday Trans.*, 1994, **90**, 1771.
6 A. P. Dickinson, H. E. O'Neal and M. A. Ring, *Organometallics*, 1991, **10**, 3513.
7 D. Sengupta and M. T. Nguyen, *Mol. Phys.*, 1996, **89**, 1567.
8 P. N. Skancke, D. A. Hrovat and W. T. Borden, *J. Am. Chem. Soc.*, 1997, **119**, 8012.
9 M. T. Nguyen, A. Dransfeld, L. Landuyt, L. G. Vanquickenborne and P. v. R. Schleyer, *Eur. J. Inorg. Chem.*, 2000, 103.
10 M. T. Nguyen, H. Vansweevelt and L. G. Vanquickenborne, *Chem. Ber.*, 1992, **125**, 923.
11 N. J. Fitzpatrick, D. F. Brougham, P. J. Groarke and M. T. Nguyen, *Chem. Ber.*, 1994, **127**, 969.
12 M. T. Nguyen, E. Van Praet and L. G. Vanquickenborne, *Inorg. Chem.*, 1994, **33**, 1153.
13 M. J. Frisch, G. W. Trucks, H. B. Schlegel, G. E. Scuseria, M. A. Robb, J. R. Cheeseman, V. G. Zakrzewski, J. A. Montgomery, Jr., R. E. Stratmann, J. C. Burant, S. Dapprich, J. M. Millam, A. D. Daniels, K. N. Kudin, M. C. Strain, O. Farkas, J. Tomasi, V. Barone, M. Cossi, R. Cammi, B. Mennucci, C. Pomelli, C. Adamo, S. Clifford, J. Ochterski, G. A. Petersson, P. Y. Ayala, Q. Cui, K. Morokuma, D. K. Malick, A. D. Rabuck, K. Raghavachari, J. B. Foresman, J. Cioslowski, J. V. Ortiz, A. G. Baboul, B. B. Stefanov, G. Liu, A. Liashenko, P. Piskorz, I. Komaromi, R. Gomperts, R. L. Martin, D. J. Fox, T. Keith, M. A. Al-Laham, C. Y. Peng, A. Nanayakkara, C. Gonzalez, M. Challacombe, P. M. W. Gill, B. Johnson, W. Chen, M. W. Wong, J. L. Andres, M. Head-Gordon, E. S. Replogle and J. A. Pople, *Gaussian 98*, Gaussian, Inc., Pittsburgh PA, 1998.
14 M. P. Fuelscher, J. Olsen, P. A. Malmqvist and B. O. Roos, *Molcas*, version 4.0, Dept. of Theoretical Chemistry, Chemical Centre, Lund, Sweden, 1999.
15 R. G. Parr and W. Yang, *Density Functional Theory of Atoms and Molecules*, Oxford University Press, New York, 1989.
16 S. Miertus, E. Scrocco and J. Tomasi, *Chem. Phys.*, 1981, **55**, 117.
17 M. Cossi, V. Barone, R. Cammi and J. Tomasi, *Chem. Phys. Lett.*, 1996, **255**, 327.
18 M. T. Bowers, R. A. Beaudet, H. Coldwhite and R. Tang, *J. Am. Chem. Soc.*, 1969, **91**, 17.
19 S. Barach, *J. Comput. Chem.*, 1989, **10**, 392; S. Barach, *J. Phys. Chem.*, 1989, **93**, 7780 and references therein.
20 C. Schade and P. v. R. Schleyer, *J. Chem. Soc., Chem. Commun.*, 1987, 1399.
21 M. T. Nguyen, G. Raspoet and L. G. Vanquickenborne, *J. Am. Chem. Soc.*, 1997, **119**, 2552.
22 T. Veszpremi, *Adv. Mol. Struct. Res.*, 2000, **6**, 267.
23 M. T. Nguyen, A. Van Keer and L. G. Vanquickenborne, *J. Org. Chem.*, 1996, **61**, 7077.
24 M. T. Nguyen, A. Van Keer, L. A. Erkisson and L. G. Vanquickenborne, *Chem. Phys. Lett.*, 1996, **254**, 307.

25 L. Pauling, in *The Nature of the Chemical Bond*, Cornell University Press, New York, 1948, p. 53.
26 S. F. Boys, *Rev. Mod. Phys.*, 1960, **32**, 296.
27 R. G. Pearson, *Chemical Hardness*, Wiley-VCH, Weinheim, 1997.
28 P. Geerlings, F. De Proft and W. Langenaeker, *Adv. Quantum Chem.*, 1999, **33**, 303.
29 A. K. Chandra and M. T. Nguyen, *J. Phys. Chem. A*, 1998, **102**, 6181.
30 M. T. Nguyen, A. K. Chandra, S. Sakai and M. Morokuma, *J. Org. Chem.*, 1999, **64**, 65.
31 T. N. Le, L. T. Nguyen, A. K. Chandra, F. De Proft, P. Geerlings and M. T. Nguyen, *J. Chem. Soc.*, *Perkin Trans. 2*, 1999, 1249.
32 L. T. Nguyen, T. N. Le, F. De Proft, A. K. Chandra, W. Langenaeker, M. T. Nguyen and P. Geerlings, *J. Am. Chem. Soc.*, 1999, **121**, 5992.
33 R. G. Pearson and R. G. Parr, *J. Am. Chem. Soc.*, 1983, **105**, 7512.
34 T. Ghanty and S. K. Ghosh, *J. Phys. Chem.*, 1993, **97**, 4951; T. Ghanty and S. K. Ghosh, *J. Phys. Chem.*, 1996, **100**, 12295.
35 U. Hohm, *J. Phys. Chem. A*, 2000, **104**, 8418, and references therein.
36 R. Becerra and R. Walsh, *Int. J. Chem. Kinet.*, 1993, **26**, 45.
37 M. T. Nguyen, D. Sengupta and L. G. Vanquickenborne, *Chem. Phys. Lett.*, 1995, **240**, 513.